Critical Cluster Size: Island Morphology and Size Distribution in Submonolayer Epitaxial Growth

Jacques G. Amar and Fereydoon Family
Department of Physics, Emory University, Atlanta, Georgia 30322
(Received 2 June 1994)

The dynamic scaling of the island-size distribution in submonolayer epitaxial growth and its dependence on the critical island size i is studied using a realistic model of epitaxial growth for $i = 0$, 1, 2, and 3. An analytic expression for the scaled island-size distribution as a function of i is also proposed. Our results agree well with experiments on Fe/Fe(100) deposition and on Fe/Cu(100) deposition. Crossover scaling forms for the variation of the island density and critical island size as a function of temperature and deposition rate are also presented.

PACS numbers: 68.55.–a, 61.43.Hv, 82.20.Mj

Understanding the physics of epitaxial growth has been a long-standing problem in surface physics and materials science. Recently considerable theoretical [1–11] and experimental [12–22] efforts have been made to understand the kinetic processes which control the nucleation and subsequent growth of submonolayer islands in both homoepitaxial [12–17] and heteroepitaxial [18–22] systems. In these experiments, atoms are deposited onto a substrate where they diffuse and aggregate to form a distribution of islands of different sizes. One fundamental concept that has emerged from these studies is that of a critical island size i corresponding to *one less* than the number of atoms needed to form the smallest stable island. For example (see Fig. 1), depending on the bond energies, temperature, and deposition rate, one may have a situation in which monomers diffuse but dimers are stable ($i = 1$), or in which a trimer is the smallest stable island ($i = 2$), or in which the smallest stable island size corresponds to a tetramer ($i = 3$). Standard rate equation theory [1,2] predicts that for a given critical island size i, the island density N in the precoalescence regime scales as $N \sim R^{-\chi_i}$, where $R = D/F$ is the ratio of the (monomer) diffusion rate D to the deposition flux F and where $\chi_i = i/(i + 2)$. The exponent χ_i has been measured in a variety of experiments and used to determine the critical island size as well as the activation energy E_a for diffusion.

Recent experiments by Stroscio and Pierce [16], and by Chambliss and Johnson [22] have shown that the distribution of island sizes also depends sensitively on the critical island size i. Theoretical studies using both rate equations [6,11] as well as simulations of point-island models [6] where islands are assumed to be pointlike (i.e., have no spatial extent) have been carried out. However, calculations of the island-size distribution based on these models do not agree with experiments. In addition, while simulations of the island-size distribution for more realistic models (mainly for $i = 1$) have recently been carried out [7–11], no systematic study of the island-size distribution and its dependence on the critical cluster size i has so far been performed.

In this Letter, we study the dynamic scaling of the island-size distribution and its dependence on the critical island size using extensive Monte Carlo simulations of a realistic model of epitaxial growth. We also derive an analytic expression for the scaled island-size distribution as a function of i which agrees well with our simulation results as well as with experiments on Fe/Fe(100) deposition at low and high temperatures and on Fe/Cu(100) deposition at room temperature. Finally, we present a quantitative expression for the variations of the island density and critical island size with temperature and deposition rate and demonstrate that our crossover scaling results can be used to determine the transition temperature for the change in the critical island size as well as the activation energy for nearest-neighbor attachment in Fe/Fe(100).

According to the dynamic scaling assumption [23], the island-size distribution $N_s(\theta)$, corresponding to the density per site of islands containing s atoms at coverage θ, can be written in the general scaling form [3,6,8]

$$N_s(\theta) = \theta S^{-2} f_i(s/S), \tag{1}$$

where $S(\theta) = \sum_s s N_s(\theta) / \sum_s N_s(\theta)$ is the average island size and where the scaling function $f_i(u)$ satisfies the sum rules $\int_0^\infty f_i(u)\,du = \int_0^\infty f_i(u) u\,du = 1$. Our analytical expression for $f_i(u)$ is based, in part, on the observation [8] that for the case of fractal islands with $i = 1$ in the scaling regime, the island-size distribution scaling function $f_1(u)$ has approximately linear behavior for small

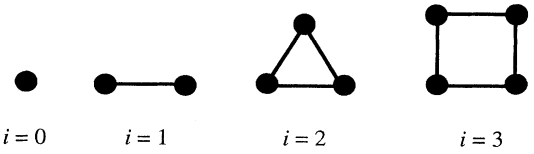

FIG. 1. Diagram showing stable island configurations for different critical island sizes $i = 0$ to 3. The case $z = 1$ corresponds to $i = 1$ on any lattice, while $z = 2$ corresponds to $i = 2$ and 3 on triangular and square lattices, respectively. Also shown is the case $i = 0$, which corresponds to freezing of monomers.

 0031-9007/95/74(11)/2066(4)$06.00

u, with both the lower limit of the linear region and $f_1(0)$ approaching zero with increasing D/F and coverage [8,24]. For $i > 1$ we expect smaller islands to have a lower density and $f_i(u)$ to go to zero faster than the first power. We therefore assume that for general i in the asymptotic large D/F limit, the island-size distribution behave as u^i for small u. Assuming a form with an exponential cutoff and a peak at $u = 1$ corresponding to the average island size, this leads to the following approximate general scaling form for $i \geq 1$:

$$f_i(u) = C_i u^i e^{-i a_i u^{1/a_i}}, \tag{2a}$$

where the constants C_i and a_i satisfy the expressions

$$\frac{\Gamma[(i+2)a_i]}{\Gamma[(i+1)a_i]} = (ia_i)^{a_i}, \quad C_i = \frac{(ia_i)^{(i+1)a_i}}{a_i \Gamma[(i+1)a_i]}, \tag{2b}$$

which are determined from the sum rules for $f_i(u)$. We note that this form is quite different from the size distribution obtained from solution of the point-island rate equations in the large D/F limit [6,7,25],

$$f_i(u) = \frac{1}{i+2}\left(1 - \frac{i+1}{i+2}u\right)^{-\frac{i}{i+1}}; \quad 0 \leq u \leq \frac{i+2}{i+1}, \tag{3a}$$

$$f_i(u) = 0; \quad u > \frac{i+2}{i+1}. \tag{3b}$$

In addition to the difference in the small-u behavior, our analytical form (2) has a peak at $u = 1$ for all i, whereas in (3) the distribution diverges at $u = (i+2)/(i+1)$.

In order to determine the scaled island-size distribution as a function of critical size i, we carried out extensive simulations of a simple but realistic model of epitaxial growth. In our model, atoms are randomly deposited on a lattice at a rate F per site per unit time. Monomers that have been deposited on the substrate or on top of an existing island diffuse by nearest-neighbor hops at a rate given by $D = D_0 e^{-E_a/k_B T}$, where E_a is the activation energy. Similarly, a surface atom with $0 < n < z$ in-plane nearest neighbors can hop with activation energy E_n so that the relative diffusion rate is given by $\tau_n = D_n/D = e^{-\Delta E_n/k_B T}$ where $\Delta E_n = E_n - E_a$. In order to study the effects of island relaxation on island morphology we have also included an additional activation energy $E_e (\tau_e = e^{-\Delta E_a/k_B T})$ corresponding to enhanced diffusion of atoms with one nearest neighbor along the edge of an island. To systematically study the effect of the critical island size on the island-size distribution we assume the atoms with z or more neighbors are not allowed to detach from an existing island. This implies that in our model, the critical island size i depends on both the underlying lattice and z (see Fig. 1). By varying z and studying various lattices as well as varying the relevant activation energies, we studied the island-size distribution and morphology for $i = 0$, 1, 2, and 3.

Figure 2(a) shows our results for the island-size distribution scaling function for the case $i = 1$, obtained from simulations on a square [8] and triangular lattice with $z = 1$ corresponding to deposition with irreversible nearest-neighbor attachment. The open squares and circles correspond to simulations without edge diffusion, which leads to fractal islands, while the open diamonds correspond to simulations of compact islands with finite edge diffusion. Also shown is our analytical form (2) for $f_1(u)$, along with experimental results for Fe/Fe(100) deposition in the temperature range 20 °C–207 °C for which the critical island size is believed to be 1 [15]. As can be seen, there is very good agreement between our simulation results and our analytical form, as well as with the Fe/Fe(100) experimental results. We note, however, that there exists a weak

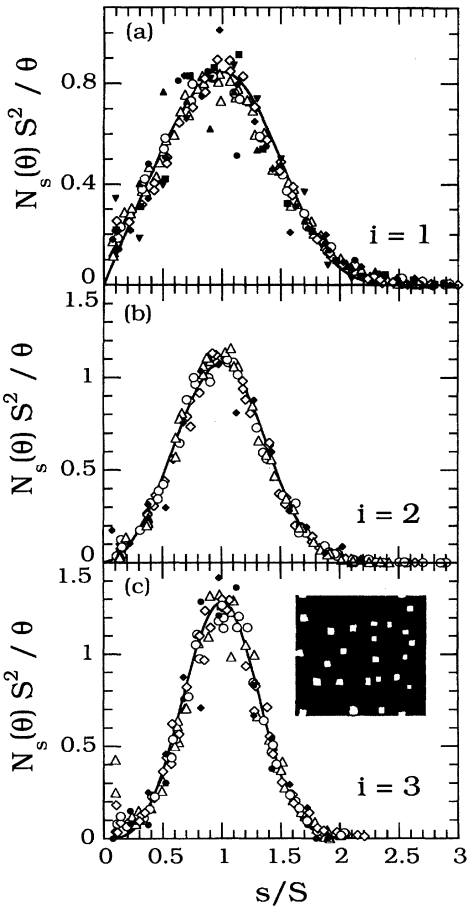

FIG. 2. Comparison of our simulation results (open symbols), analytic form Eq. (2) (solid line), and experimental results for Fe/Fe(100) (filled symbols) for the island-size distribution scaling function $f_i(u)$ for $i = 1$, 2, and 3. (a) $i = 1$. Simulation results are for $\theta = 0.1$–0.4 with $r_1 = 0$, $R = 10^8 - 10^9$, and $r_e = 0$–10^4. Experimental data [16] are for $T = (20$–$207)$ °C. (b) $i = 2$. Simulation results are for $\theta = 0.1$–0.4, $R = 10^7 - 10^8$, and $r_1 = 0.003$–1. Filled diamonds are the experimental results at $T = 250$ °C. (c) $i = 3$. Simulation results on a square lattice for $\theta = 0.06$–0.3 with $R = 5 \times 10^9 - 10^{11}$, $r_1 = 10^{-4}$–2.5×10^{-6}, and $r_e = 0$–10^{-2}. Experimental results are for $T = 301$ °C (diamonds) and $T = 356$ °C (circles). Inset shows picture of island from simulations at $\theta = 0.06$ for the case $R = 5 \times 10^9$, $r_1 = 10^{-4}$ with $r_e = 0$ and $N = 6.7 \times 10^{-5}$.

dependence of the island-size distribution scaling function on the island morphology for small u [24], since for fractal islands $f_1(0)$ goes to zero with increasing D/F, while for compact islands $f_1(0)$ remains finite at low coverage. However, with increasing coverage the compact distribution appears to approach the fractal distribution and our analytical form.

The case $i = 2$ was simulated on a triangular lattice with the restriction that any atom with two or more nearest neighbors is irreversibly "frozen" (i.e., $z = 2$). Figure 2(b) shows our simulation results are in good agreement with our analytic form (2) for $i = 2$. A log-log plot of the data [24] for small u has slope 2.05 ± 0.05, in agreement with our conjecture for the small u behavior of $f_2(u)$. The filled diamonds shown in Fig. 2(b) are experimental results for Fe/Fe(100) at an intermediate temperature $T = 250\,^{\circ}\mathrm{C}$ which demonstrate that with increasing temperature the critical island size crosses over to a higher value.

The case $i = 3$ has been suggested as the critical cluster size for Fe/Fe(100) deposition at elevated temperatures [16], since at these temperatures the probability for an atom with one nearest neighbor to detach from an island becomes significant while the probability for an atom with two nearest neighbors to detach is negligible. In this case the minimal stable configuration is a tetramer (see Fig. 1) and we studied a similar model for $i = 2$ but on a square lattice. As can be seen in Fig. 2(c), the simulation results (both with and without enhanced edge diffusion) cover a wide range of coverages, as well as values of D/F and r_1, including $\theta \simeq 0.07$ for which the island-size distribution was measured for Fe/Fe(100). There is, again, very good agreement between all our simulation results and the analytical form (2) as well as the experiments. This confirms that $i = 3$ is the critical island size for Fe/Fe(100) deposition [16] in the temperature range 301 °C–356 °C. In addition, a log-log plot of our simulation results for small u [24] gives $f_3(u) \sim u^x$, with $x \simeq 2.9$, in good agreement with our conjecture for the small-u behavior of $f_3(u)$. The inset in Fig. 2(c) shows a typical picture of the islands formed at an island density close to that observed in the experiments.

In addition to $i = 1$ to 3, we also considered the case $i = 0$ which corresponds to the spontaneous nucleation or freezing of monomers. This may occur due to the presence of surfactants or impurities on the surface [14] and has also been experimentally observed in the case of Fe on Cu(100) deposition [22]. In this case isolated Fe atoms spontaneously embed into the substrate and form stable islands leading to a critical island size $i = 0$. As shown by Chambliss and Johnson, using a rate-equation approach, this implies $\chi_0 = 0$ (i.e., the island density is independent of D/F), in agreement with the prediction $\chi_i = i/(i + 2)$. To simulate this case, we studied a model in which (in addition to the usual diffusion with hopping rate D), monomers spontaneously freeze and form stable islands at a rate given by $R_s = r_s D$, where $r_s = e^{-\Delta E_s/k_B T}$ depends on the extra activation energy $\Delta E_s = E_s - E_a$ beyond that for normal diffusion. In addition, any monomers that become nearest neighbors of an embedded island are immediately added irreversibly to the embedded island. Figure 3 shows our results for the island-size distribution scaling function for this case for $r_s = 10^{-3} - 10^{-5}$ and $\theta = 0.06 - 0.3$ and $D/F \geq 10^9$. The island-size distribution scaling function f_0 is essentially independent of the embedding probability ratio r_s as well as D/F for large D/F over all coverage. As expected from our conjecture for the small-u behavior of $f_i(u)$, the island-size distribution scaling function in this case is nonzero at $u = 0$. In addition, the scaling function looks quite similar to that obtained in the experiment. However, there does not seem to be a simple analytic form for $f_0(u)$.

Finally, we made a systematic study of the variation of the island density N and critical island size i with temperature, which is important in the interpretation of experiments. For fixed values of the critical island size i, our simulation results ($\chi_0 \simeq 0$, $\chi_1 = 0.33$, $\chi_2 = 0.5$, and $\chi_3 \simeq 0.58$) are in good agreement with the rate-equation prediction $\chi_i = i/(i + 2)$. By varying r_1 and $R = D/F$, which is equivalent to varying the temperature, we studied the crossover from $i = 1$ to $i = 2$ on a triangular lattice and from $i = 1$ to $i = 3$ on a square lattice. For example, for simulations on a square lattice with large R and finite r_1 and island densities in the range of those observed for Fe/Fe(100) at high temperatures, we find $N \sim R^{-\chi_3} r_1^{-0.33}$ with $\chi_3 \simeq 0.6$ corresponding to $i = 3$. However, for smaller R or very small r_1, we find a crossover to $\chi_1 = \frac{1}{3}$, corresponding to $i = 1$. Our results for the crossover in the critical island size from $i = j$ to $i = k$ can be summarized by the general scaling form for the island density as a function of r_1 and R:

$$N(r_1, R) = R^{-\chi_j} f_{jk}(r_1^{x_{jk}} R), \tag{4}$$

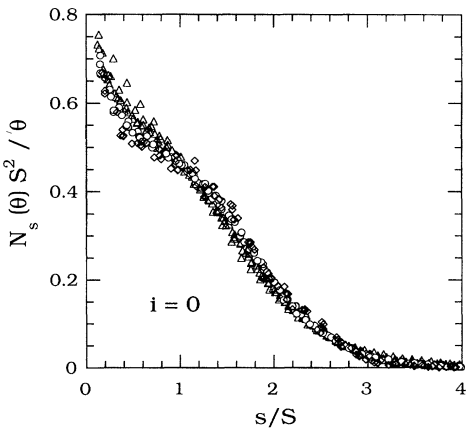

FIG. 3. Island-size distribution scaling function $f_0(u)$ from simulations on a square lattice for $i = 0$ with $r_s = 10^{-3}$ (triangles), 10^{-4} (circles), and 10^{-5} (diamonds) with $R \geq 10^9$.

where $f_{jk}(u) \sim$ const for $u \ll 1$, and $f_{jk}(u) \sim u^{\chi_j - \chi_k}$ for $u \gg 1$. We find $x_{12} \simeq 1.5$ and $x_{13} \simeq 1.25$. Using the scaling form (4) as well as our simulation results for the crossover scaling function f_{13} [24] and comparing with the experimental value of the island density and D/F at $T = 356\,^{\circ}\mathrm{C}$ given in Ref. [15], we have estimated the activation energy ΔE_1 for "one-bond" detachment in Fe/Fe(100). We find $\Delta E_1 = 0.6 \pm 0.1$ eV in good agreement with a previous experimental estimate of 0.55 eV [16] as well as with a recent estimate (0.7 eV) based on a rate-equation analysis [26]. Surprisingly, this number is much larger than might be expected from bond counting and cohesive energy arguments [27]. Thus it may correspond to an "effective" dissociation energy arising from complex kinetic processes [26]. An alternate possibility [28] is that the large value of ΔE_1 stems from the existence of two different diffusion mechanisms (e.g., exchange and hopping) which have different activation energies. This possibility was not included in our simulations. A complete understanding of the meaning of this large value will require detailed first-principle calculations.

We may also use the previously estimated values of D_0 and E_a [15] along with our crossover scaling results to estimate the *transition temperature* T_x from $i = 1$ to $i = 3$ behavior in Fe/Fe(100) deposition. We find $T_x = 260\,^{\circ}\mathrm{C} - 300\,^{\circ}\mathrm{C}$ where the lower limit corresponds to the onset of deviations from $i = 1$ behavior and the upper limit corresponds to full-blown $i = 3$ behavior, in good agreement with the experimental results shown in Fig. 2.

In conclusion, we have carried out extensive simulations of a realistic model of submonolayer epitaxial growth. Our results for the scaled island-size distribution for critical island size $i = 0$, 1, 2, and 3 demonstrate clearly the strong dependence on critical island size and are in good agreement with recent experiments. We have also proposed an analytic form for the scaled island-size distribution $f_i(u)$ based on the small-u behavior as well as well-known sum rules which gives excellent agreement for $i = 1 - 3$ both with experiments and with our simulations. Finally, we have presented a quantitative discussion of the variation of the island density and critical island size as functions of temperature and deposition rate. We expect that our analytical and simulation results for the island-size distribution as well as our crossover scaling results will be useful in the analysis of a wide variety of experiments on submonolayer epitaxial growth.

This work was supported by National Science Foundation Grant No. DMR-9214308 and by the Office of Naval Research. We thank David Chambliss, Jim Evans, Joseph Stroscio, and Andy Zangwill for useful discussions. We would like to thank Joseph Stroscio for providing us with the experimental island-size distribution data for Fe/Fe(100) and David Chambliss for a preprint of Ref. [22]. Part of this work was carried out using the computational facilities of the Cherry L. Emerson Center for Computational Science at Emory University.

[1] J. A. Venables, G. D. Spiller, and M. Hanbucken, Rep. Prog. Phys. **47**, 399 (1984).
[2] S. Stoyanov and D. Kashchiev, in *Current Topics in Materials Science,* edited by E. Kaldis (North-Holland, Amsterdam, 1981), Vol. 7, pp. 69–141.
[3] F. Family and P. Meakin, Phys. Rev. Lett. **61**, 428 (1988); Phys. Rev. A **40**, 3836 (1989).
[4] J. Villain, A. Pimpinelli, L. Tang, and D. Wolf, J. Phys. I (France) **2**, 2107 (1992); J. Villain, A. Pimpinelli, and D. Wolf, Comments Cond. Mat. Phys. **16**, 1 (1992).
[5] L.-H. Tang, J. Phys. I (France) **3**, 935 (1993).
[6] M. C. Bartelt and J. W. Evans, Phys. Rev. B **46**, 12 675 (1992).
[7] M. C. Bartelt and J. W. Evans, Surf. Sci. **298**, 421 (1993); J. W. Evans and M. C. Bartelt, J. Vac. Sci. Technol. A **12**, 1800 (1994).
[8] J. G. Amar, F. Family, and P.-M. Lam, Phys. Rev. B **50**, 8781 (1994).
[9] C. Ratsch, A. Zangwill, P. Smilauer, and D. D. Vvedensky, Phys. Rev. Lett. **72**, 3194 (1994).
[10] G. T. Barkema, O. Biham, M. Breeman, D. O. Boerma, and G. Vidali, Surf. Sci. Lett. **306**, L569 (1994).
[11] G. S. Bales and D. C. Chrzan, Phys. Rev. B **50**, 6057 (1994).
[12] H. J. Ernst, F. Fabre, and J. Lapujoulade, Phys. Rev. B **46**, 1929 (1992).
[13] E. Kopatzki, S. Gunther, W. Nichtl-Pecher, and R. J. Behm, Surf. Sci. **284**, 154 (1993).
[14] G. Rosenfeld, R. Servaty, C. Teichert, B. Poelsema, and G. Comsa, Phys. Rev. Lett. **71**, 895 (1993).
[15] J. A. Stroscio, D. T. Pierce, and R. A. Dragoset, Phys. Rev. Lett. **70**, 3615 (1993).
[16] J. A. Stroscio and D. T. Pierce, Phys. Rev. B **49**, 8522 (1994).
[17] J.-K. Zuo, J. F. Wendelken, H. Durr, and C.-L. Liu, Phys. Rev. Lett. **72**, 3064 (1994).
[18] Y. W. Mo, J. Kleiner, M. B. Webb, and M. G. Lagally, Phys. Rev. Lett. **66**, 1998 (1991).
[19] J.-K. Zuo and J. F. Wendelken, Phys. Rev. Lett. **66**, 2227 (1991).
[20] R. Q. Hwang, J. Schroder, C. Gunther, and R. J. Behm, Phys. Rev. Lett. **67**, 3279 (1991); R. Q. Hwang and R. J. Behm, J. Vac. Sci. Technol. B **10**, 256 (1992).
[21] W. Li, G. Vidali, and O. Biham, Phys. Rev. B **48**, 8336 (1993).
[22] D. D. Chambliss and K. E. Johnson, Phys. Rev. B **50**, 5012 (1994).
[23] T. Vicsek and F. Family, Phys. Rev. Lett. **52**, 1669 (1984).
[24] J. G. Amar and F. Family (to be published).
[25] F. Family and J. G. Amar, Mater. Sci. Eng. B (Solid State Mat.) (to be published).
[26] M. C. Bartelt, L. S. Perkins, and J. W. Evans (to be published).
[27] P. J. Feibelman (private communication).
[28] P. J. Feibelman (to be published).